

Spring 5-2012

The Ages and Metallicities of Type Ia Supernova Host Galaxies from the Nearby Galaxies Supernova Search Program

Suzanna Sadler

Western Kentucky University, suzanna.sadler347@topper.wku.edu

Follow this and additional works at: http://digitalcommons.wku.edu/stu_hon_theses



Part of the [Stars, Interstellar Medium and the Galaxy Commons](#), and the [The Sun and the Solar System Commons](#)

Recommended Citation

Sadler, Suzanna, "The Ages and Metallicities of Type Ia Supernova Host Galaxies from the Nearby Galaxies Supernova Search Program" (2012). *Honors College Capstone Experience/Thesis Projects*. Paper 356.
http://digitalcommons.wku.edu/stu_hon_theses/356

This Thesis is brought to you for free and open access by TopSCHOLAR®. It has been accepted for inclusion in Honors College Capstone Experience/Thesis Projects by an authorized administrator of TopSCHOLAR®. For more information, please contact topscholar@wku.edu.

THE AGES AND METALLICITIES OF TYPE IA SUPERNOVA HOST GALAXIES
FROM THE NEARBY GALAXIES SUPERNOVA SEARCH PROGRAM

A Capstone Experience/Thesis Project

Presented in Partial Fulfillment of the Requirements for

the Degree Bachelor of Science with

Honors College Graduate Distinction at Western Kentucky University

By

Suzanna M. Sadler

* * * * *

Western Kentucky University
2012

CE/T Committee:

Dr. Louis-Gregory Strolger

Dr. Michael Carini

Dr. Walter Collett

Approved by

Advisor

Department of Physics & Astronomy

Copyright by
Suzanna Marie Sadler
2012

ABSTRACT

We seek to better understand the physical constraints under which White Dwarf stars ultimately become Type Ia supernovae (SNe Ia), an important test of the robustness of these tools in precisely measuring Dark Energy, as the definite progenitor system still remains elusive. The host galaxy environments of Type Ia supernovae provide our best opportunity for constraining the mechanism(s) of SN Ia production, i.e., the stars involved and the incubation times (tied to stellar ages), and the sensitivity of SNe Ia to changes in the local metallicity. We have measured the ages and metallicities of approximately 60 galaxies from a sample of Type Ia supernova hosts collected by the Nearby Galaxies Supernova Search project. In this manuscript, I present the completed analysis on 16 of these host galaxies, comparing their optical spectral data to synthesized galaxy models (from single stellar populations) to determine the dominant stellar ages and metallicities. Evidence shows a stronger dependence on the age of the host than the host's metallicity, apparently conflicting with some predictions. These results are puzzling, but preliminary. A full analysis on all host data, and perhaps with more complex models, will provide a validity test of the mostly indirect trends established in other low- z surveys (e.g. Sloan Digital Sky Survey), and may ultimately steer future investigations for more precise SN Ia cosmology.

Keywords: Astrophysics, Dark Energy, Supernovae, Galaxies, Stellar Populations

Kurt,
It's only the beginning, love.

Dad,
What is it like seeing the stars from up there?

Mom,
There is nowhere I can go where your prayer has not already been.

Katherine,
Thank you for teaching me to never look down on a sister except to pick her up.

Victoria,
If life was a cookie, you would definitely be the chocolate chips.

ACKNOWLEDGEMENTS

This work would not have been possible without the exceptional support from countless people. I must thank my advisor, Dr. Louis Strolger for all of the time, effort, patience, dedication, and forgiveness that it took to get me to this point. I also wish to thank the Department of Physics & Astronomy as a whole for their effort in giving students exceptional support, mentorship, and opportunities. I would also like to acknowledge the numerous people who contributed to my project in various, though indispensable ways: Schuyler Wolff, Andrew Gott, and April Pease, along with all of the by-capture proofreaders. There were countless contributions to this work in other ways that I'll never know. Thank you all.

Additional acknowledgments to Western Kentucky University's Ogden College and Honors College for financial support throughout my career. Funding for my project also came from a scholarship through the Kentucky Space Grant Consortium.

VITA

May 20, 1991	Born - Murray, Kentucky
2009	Carol M. Gatton Academy of Mathematics and Science, Bowling Green, Kentucky
2009	Trigg County High School, Cadiz, Kentucky
2010	Pi Mu Epsilon (ΠΜΕ) inductee
2010	<i>Department of Physics and Astronomy</i> <i>Rookie of the Year Award</i>
2010 - 2011	Kentucky Space Grant Consortium Undergraduate Scholar
2011	<i>Randall Harper Award for Outstanding Research in Physics and Astronomy</i>
2011	Sigma Pi Sigma (ΣΠΣ) inductee
2011 - 2012	President, Society of Physics Students, WKU chapter
2012	<i>Dr. George V. and Sadie Skiles Page Award for Excellence in Scholarship,</i> Physics and Astronomy

PUBLICATIONS

1. **Sadler, S. M.**, Strolger, L., & Wolff, S. 2011, Bulletin of the American Astronomical Society, 43, #337.14
2. **Sadler, S. M.**, Strolger, L., Wolff, S., & Gott, A. 2011, National Conference on Undergraduate Research, Ithaca College, Ithaca, NY
3. Strolger, L.-G., van Dyk, S., Wolff, S., Campbell, L., **Sadler, S. M.**, & Pease, A. 2011, NOAO Proposal ID #2011A-0416, 416
4. Wolff, S., Strolger, L.-G., & **Sadler, S. M.** 2011, National Conference on Undergraduate Research, Ithaca College, Ithaca, NY
5. **Sadler, S. M.**, Strolger, L., Wolff, & S. 2010, Southeastern Section of the American Physical Society, Louisiana State University, Baton Rouge, LA

FIELDS OF STUDY

Major Field: Physics

Minor Field: Astronomy, Mathematics

TABLE OF CONTENTS

ABSTRACT	ii
ACKNOWLEDGEMENTS	iv
LIST OF FIGURES	vii
LIST OF TABLES	ix
CHAPTER	
I. Background and Introduction	1
1.1 Supernovae: An Introduction	2
1.2 Why Study Supernovae?	4
1.3 Delay-Time Distribution of Type Ia Supernovae: An Issue of Metallicity or Age?	6
1.4 The Delay Time Distributions	9
II. Data: Groundwork to Present	12
2.1 Groundwork: The Nearby Galaxies Supernova Search Project	12
2.2 Host Galaxy Spectra: Kitt Peak & Palomar	14
III. Tests of Environmental Effects	17
3.1 Determination of Metallicity and Ages in the Sample	17
3.1.1 The MILES Templates	19
3.1.2 The Inadequacies of EZ_Ages	19
3.1.3 The CC-Test	21
IV. Conclusions	26
4.1 Results & Discussion	26
4.1.1 Table of Ages and Metallicities	28
4.1.2 Future Work	28
BIBLIOGRAPHY	32

LIST OF FIGURES

Figure

1.1	From Filippenko 1997, examples of spectral differences between types of supernovae.	3
1.2	H-R diagram of stars in the Solar neighborhood, from the Hipparcos catalog (grey points, Perryman et al. 1997). Red lines indicate <i>isochrones</i> , or lines of stars of the same stellar age (annotated on diagram). Stars spend nearly 90% of their lifetimes on the Main Sequence, in the large group of stars that extend from upper left to lower right of the diagram. From there they begin a quick death process that pauses in the Red Giant phase (grouping in the upper right), and for many culminates as supernovae. The age describes the isochrone, and the mass is the turnoff point of the particular isochrone.	7
2.1	Sky coverage for the Nearby Galaxies Supernova Search. Each box indicates a single pointing of the 0.9m + Mosaic (~ 1 square degree) and are color coded by epoch, or visit. Gray is the template, blue is the second epoch, red is the third epoch, and purple is the fourth epoch.	13
3.1	Spectrum of host galaxy of SN 1999av. This spectrum shows strong absorption features – Lick Indices – which passively tell about the chemical enrichment and ages of stars in the galaxy.	18
3.2	Plot of errors calculated between input parameters and parameters measured by EZ_Ages. Colors are based on error percentages of the greatest error (either age or metallicity, indicated in each box). Green boxes indicate errors below 20%, yellow boxes indicate errors between 20% and 50%. Red boxes are 100% errors, or failures. These are combinations that EZ_Ages could not output a measure of age or metallicity.	20
3.3	Illustration of the Minimum- χ^2 fit method between data and a MILES template spectrum. This plot shows a model that poorly fits the data, shown by its larger residuals in χ space.	22

3.4	Illustration of the Minimum- χ^2 fit method between data and a MILES template spectrum. This plot shows a model that is a better fit to the data. The residuals in this comparison are much smaller than Figure 3.3.	23
3.5	Illustration of the Minimum- χ^2 fit method between data and a MILES template spectrum. This plot shows a model that returned to be the minimum- χ^2 for the data for SN 1999ep. The residuals in χ space are the smallest out of every possible combination.	24
3.6	Contour plot, showing contour regions. The age and metallicity ranges were determined by analyzing the darkest region. The white region shows the untested region due to lack of MILES spectra.	25
4.1	Final plot with an estimation of Meng's prediction region overlaid. Upper left of the plot would include young, star-forming galaxies. Upper right of the plot would include old, star-forming galaxies. Bottom left of the plot would be unusual galaxies – young, but lacking in the metal content that one would expect with the increased metal abundances in the universe (Note that this region was generally untestable due to the lack of MILES spectra). Bottom right of the plot would contain old, dying red galaxies that did not undergo many phases of star-formation.	27

LIST OF TABLES

Table

2.1	<i>NGSS</i> Supernovae and revisit-discovered supernovae used in Age/Metallicity comparison.	16
4.1	Numerical findings from Age/Metallicity comparison.	28

CHAPTER I

Background and Introduction

Dark energy is a pervasive, repulsive force that makes up about 75% of the energy in the universe. The idea of Dark Energy has roots in the work of Albert Einstein and Edwin Hubble and proof of its existence has culminated in a Nobel Prize in Physics. The discovery of Dark Energy leaves in its wake a puzzle, a problem, and a scandal.

The Dark Energy Puzzle: Dark Energy exists! What is the nature of this energy that seems to dominate the universe?

The Probing Problem: Type Ia supernovae are the best tools to measure the nature of Dark Energy, but we don't know why these tools work (i.e. the physics behind their mechanisms).

The Progression Scandal: Type Ia supernovae may be a diverse set of events, with a diverse set of progenitor mechanisms, which would cast doubt on our ability to use them uniformly to measure the nature of Dark Energy. And, so, we are back to square one.

We must better understand Type Ia supernovae to be confident in our measurements of the nature of Dark Energy. This requires probing the environments of these events to better

constrain the physical mechanisms behind their production.

1.1 Supernovae: An Introduction

Supernovae (SNe) are the catastrophic deaths of certain stars as they explode and expel mass and energy into space. On average, these events occur once every 100 to 500 years in typical galaxies like our Milky Way (Wolff 2010) and last on the order of a few months to a year. All supernova events can be placed in one of two physical categories – thermonuclear or kinematic – based on their differences in basic mechanisms. However, they are categorized based on characteristics in their optical spectra (See Figure 1.1). In summary, Type I SNe are distinguished from Type II SNe by their absence of Hydrogen lines. Within the category of Type I supernovae are three subcategories – Ia (with prominent silicon features), Ib (with prominent helium features), and Ic (with neither helium nor silicon features).

Types Ib, Ic and Type II events all have similar kinematic origins. These “core-collapse” events are the result of massive stars that have used up the fuel within their cores, leaving only iron, which has the highest binding energy per nucleon of any element. At that point, there is insufficient radiation pressure to support the gravitational pressure, and the star collapses. The collapse is abruptly halted by newly formed neutron degenerate Fe-core, and a shockwave forms as rebounding material propagates back through the in-falling material. Neutrinos are produced in the prompt nuclear burning event that explosively expels matter into space. The core-collapse event mechanism is supported by detailed numerical modeling, and recent deep archival imaging from Hubble Space Telescope have routinely shown the massive ($> 8 M_{\odot}$) stellar progenitors of these events prior to explosion. (Van Dyk, S.

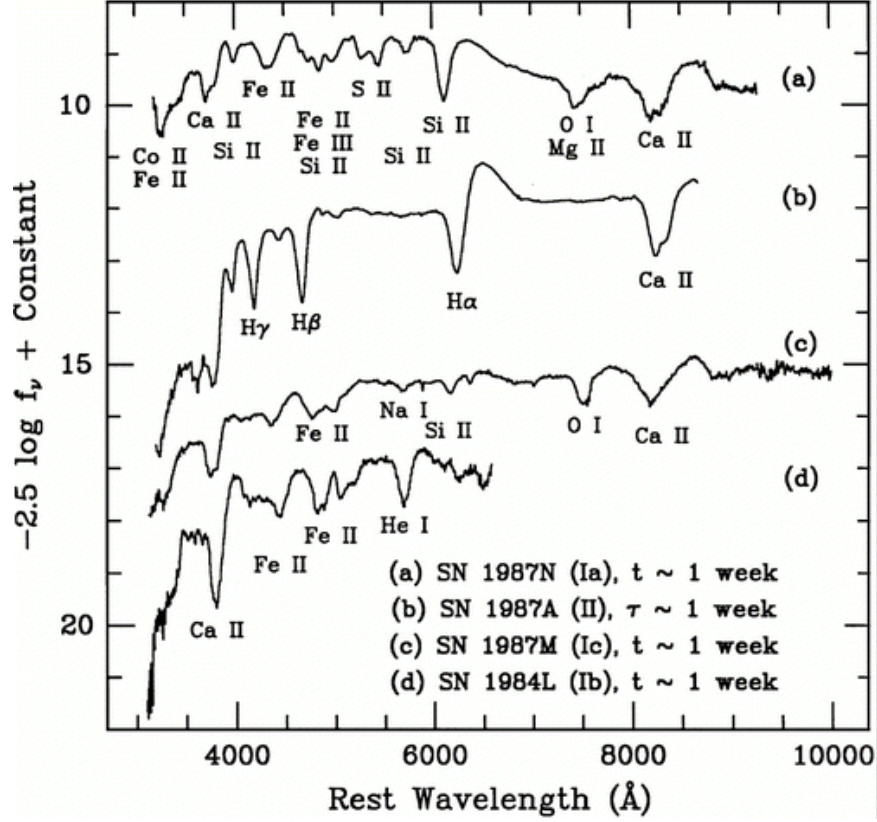


Figure 1.1: From Filippenko 1997, examples of spectral differences between types of supernovae.

D., Li, W., & Filippenko, A. V. 2003)

By contrast, Type Ia supernovae (SNe Ia) are not as well understood as the core-collapse events, partly because their progenitors have never been observed prior to explosion. It is generally accepted that SNe Ia are thermonuclear events stemming from C+O White Dwarf (WD) stars, the remnant of intermediate mass ($\sim 3 - 8 M_{\odot}$) stars that have completed the normal life cycle and have ceased nuclear fusion. In this scenario White Dwarfs are capable of further highly exothermic fusion reactions if their temperatures rise high enough to burn carbon and oxygen to Fe-peak elements. This is believed to be achieved through a process of mass accretion from a neighboring star, and culminates once the WD's mass exceeds the $1.4 M_{\odot}$ Chandrasekhar Mass Limit. Based on Jean's mass and Fragmentation arguments,

it is generally held that the companion star is roughly the same in zero-age main sequence mass as the primary, just a little delayed in evolution. Therefore, the companion is thought to be a Red Giant.

As the progenitor star mass limit is fixed, they all have a fixed maximum intrinsic brightness of $M_B \cong -19.5 \pm 0.2$, corresponding to total energy outputs of around 1×10^{44} Watts. (In one second, this event would power the entire world for roughly 10^{23} years!). The consistency of luminosity makes these events excellent standard candles and excellent probes of vast cosmic distances via the inverse square law, as shown in Equation 1.1.

$$(1.1) \quad d_L = \sqrt{\frac{L}{4\pi F}}$$

where L is the intrinsic luminosity and F is the absorption-free peak flux observed for the event. In cosmological terms, this is:

$$(1.2) \quad d_L = \frac{(1+z)}{H_0} \int_0^{z_1} \frac{1}{\sqrt{(1+z)^2(1+\Omega_M z) - z(2+z)\Omega_\Lambda}} dz$$

where the d_L is sensitive to the density of matter (Ω_M) and the density of dark energy (Ω_Λ) in a Euclidean (flat) universe where z is the redshift and H_0 is the Hubble Constant. As other astrophysical information tells the density of ordinary and dark matter in the universe, standard candle distances of SNe Ia provide excellent probes of Dark Energy.

1.2 Why Study Supernovae?

Type Ia supernovae have proven to be excellent standardizable candles, accurate to within 7% for measuring the expansion history of the universe (Phillips 1993) and using Equation 1.2, astronomers have uncovered a large Dark Energy component (Riess et

al. 1998). However, there is great uncertainty on the details of the physical mechanism by which White Dwarfs turn into SNe Ia, much of which hinges on the type of mass-donor stars involved (or more specifically, their ages), and the rate of mass accretion (governed by the chemical composition of the White Dwarf [Pinto & Eastman 2000; Timmes et al. 2003; Meng et al. 2011]). The Delay-Time Distribution, or incubation time from stellar birth to supernova event, was thought to be a way to help resolve the uncertainty in possible progenitor systems. However, Maoz et al. (2011), Sullivan et al. (2006), and Strolger et al. (2010) found largely inconsistent results. Further discussion on Delay-Time can be found in Section 1.3.

The crux of the “scandal” is the uncertainty in Type Ia Supernovae as a Dark Energy measuring tool. Investigators have found that there are numerous ways to make a SN Ia from a WD, and perhaps nature utilizes them all, but the amazing uniformity of these events is perplexing. The “canonical” model (White Dwarf + Red Giant) has an implied dependence on metallicity. Models suggest (Timmes et al. 2008) metal rich progenitors will be less luminous SNe Ia, perhaps in a way which invalidates the SN Ia standardization. What is worse, due to stellar evolution, metal abundances decrease substantially with look-back time, making SNe Ia now inherently different from SNe Ia in the distant past. It will necessarily make it tough to measure the strength or evolution in Dark Energy.

Other models (Strolger et al. 2010; Meng et al. 2011) suggest a much less massive, longer-lived companion, like a Sub-Giant or Main Sequence star. These models infer a progenitor that is less susceptible to local metallicity variations as this is “locked in” at very early epochs of the universe. Here, SNe Ia at $z \sim 0.1$ are no different from SNe Ia at $z \sim 1.0$, and thus their standard candle distances can be used to probe Dark Energy accurately and robustly. It is, therefore, extremely important to determine which is the

actual mechanism (or companion) White Dwarfs use to make SNe Ia.

Environments, specifically the ages of stars and the metallicity of stars and gas, provide some constraint on the properties of White Dwarf systems, and can be inferred from galaxy-global properties such as morphological type, luminosity, and color (Hamuy et al. 2000; Gallagher et al. 2008; Howell et al. 2009), but thus far the results have been inconclusive. However, these properties can be more accurately measured in a more direct, albeit time-consuming, method of spectroscopic measurement and matching to galaxy models, through indices of ions or molecules, or full spectrum cross-correlation. I have conducted a census of environments for a sample of low-redshift host galaxies taken from the NGSS, matching to Vazdekis MILES SSP models via cross-correlation and least-square fits, to constrain the ages and metallicities of hosts in our sample.

1.3 Delay-Time Distribution of Type Ia Supernovae: An Issue of Metallicity or Age?

It is generally agreed that the progenitor star of SNe Ia is a carbon-oxygen White Dwarf. However, there is no clear observation that indicates how the extra mass gets close enough to the White Dwarf for it to incorporate into the star and ignite carbon burning. The question now lies with the progenitor system; is it singly degenerate or doubly degenerate? That is, does the White Dwarf accrete mass from a binary companion (Main Sequence or Red Giant star), or do two White Dwarf stars merge?

One way to test the progenitor systems of these events is to investigate the Delay-Time Distribution (DTD). The “delay-time” is the time elapsed between a given star’s birth and its supernova event, and the DTD tells us about the range of progenitor system through well-established relationships between basic stellar quantities. Figure 1.2 is the Hertzsprung-

Russell (HR) Diagram, a plot depicting the relationships between luminosity, surface temperature, and mass of stars. There are a few fundamental relationships that we can determine from this diagram.

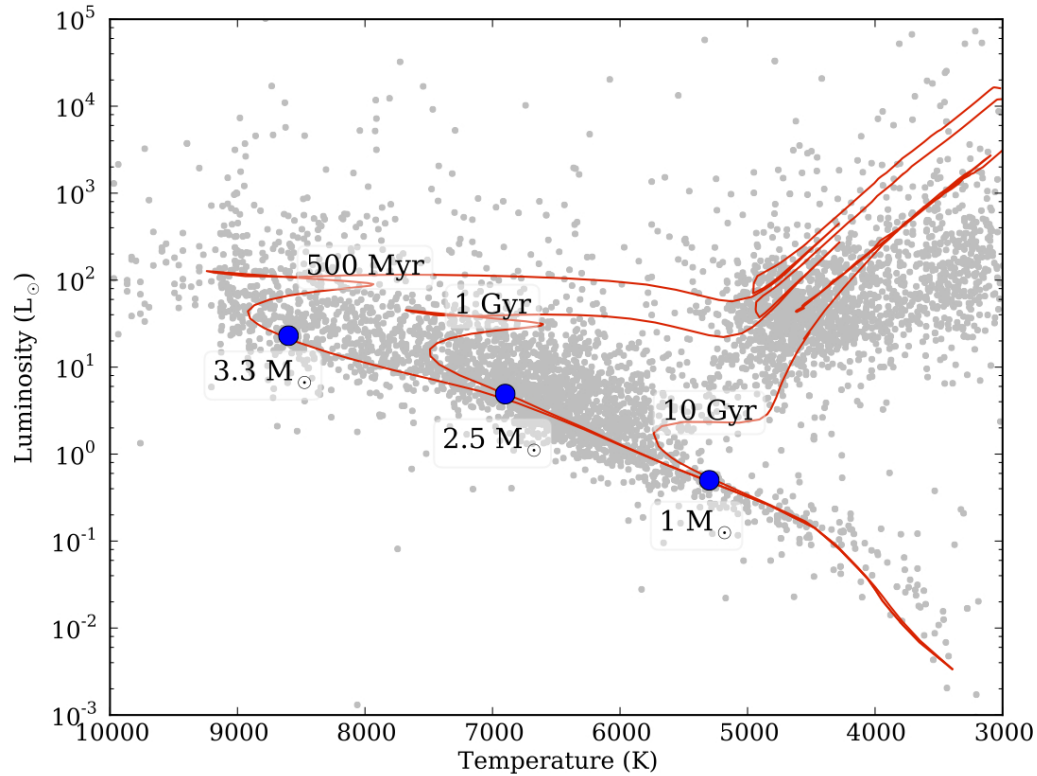


Figure 1.2: H-R diagram of stars in the Solar neighborhood, from the Hipparcos catalog (grey points, Perryman et al. 1997). Red lines indicate *isochrones*, or lines of stars of the same stellar age (annotated on diagram). Stars spend nearly 90% of their lifetimes on the Main Sequence, in the large group of stars that extend from upper left to lower right of the diagram. From there they begin a quick death process that pauses in the Red Giant phase (grouping in the upper right), and for many culminates as supernovae. The age describes the isochrone, and the mass is the turnoff point of the particular isochrone.

First, stars occupying the “Main Sequence,” the group of stars extending from the upper left to lower right of the HR Diagram (Figure 1.2), are all in hydrostatic equilibrium and are constantly nuclear burning hydrogen into helium in their cores. More massive Main

Sequence stars burn through their fuel more rapidly, but they also have more fuel to burn. Through hydrostatic equilibrium equations, one can derive the relationship between stellar mass and luminosity for stars on the main sequence, which is:

$$(1.3) \quad L \propto M^{3.5}$$

This equation shows that even a slight change in stellar mass can dramatically affect the luminosity. Massive stars have greater gravitational compression in their cores due to the sheer weight of the overlying layers; it follows that low-mass stars have a lower gravitational compression in their cores. The massive stars, therefore, need greater thermal and radiation pressure pushing outward to balance the greater gravitational compression to put the star into hydrostatic equilibrium. The greater thermal pressure is provided by the higher temperatures in the massive star's core. Simply put, more massive stars need higher core temperatures to be stable. Equation 3.1 can be written in terms of the mass and luminosity of our Sun as follows:

$$(1.4) \quad \frac{L}{L_{\odot}} = \left(\frac{M}{M_{\odot}} \right)^{3.5}$$

where L_{\odot} and M_{\odot} denote the luminosity and mass of our Sun, respectively.

This relation also gives an estimate of the lifetimes of stars of different masses. The luminosity directly tells how quickly a given star consumes its mass. In a given time (t) it will then consume a certain amount of its hydrogen fuel (M).

$$(1.5) \quad L \times t = M$$

As this rate of consumption is proportional to the amount of fuel (Equations 1.3 and 1.4), we can estimate the time it would take to consume all of its fuel by substituting into Equation 1.5

$$(1.6) \quad M^{3.5} t \propto M$$

and simplification yields the relationship between time and mass:

$$(1.7) \quad t \propto M^{-2.5}$$

Equation 1.7 tells us that as the mass of the progenitor star increases, the time it takes to go through the H-burning phase of its life, the Main Sequence lifetime, decreases nearly quadratically. Granted, stars do not consume all of their H mass in the H-burning phase, but they surprisingly eat about the same proportion of their total mass ($\sim 10\%$) making the proportionality valid for all Main Sequence stars. More over, the main sequence lifetime of a star accounts for the vast majority of the total stellar lifetime ($\sim 80\% - 90\%$ of the total time from birth to death). Therefore, it is a remarkably suitable to approximation of the longevity of stars, as illustrated in Figure 1.2.

1.4 The Delay Time Distributions

In single-degenerate SN Ia progenitor systems, the Main Sequence lifetime of the companion stars largely dictate the Delay Time of the events. Simply, the White Dwarf must wait until its companion has evolved to a point where it can donate material to the White Dwarf. This criterion is generally met when the companion leaves the Main Sequence H-burning stage. At this point, the star expands as it moves toward the Red Giant phase, and

its surface gravity is greatly reduced, allowing for mass transfer. By contrast, in double-degenerate systems, the Delay Time is governed by the angular momentum of the WD+WD pair, the initial separation, and the time necessary to gravitationally radiate away the angular momentum to “spin up” to collision.

In principle, each system (WD+MS, WD+RG, WD+WD) would have an inherent distribution of Delay Times, based either on the allowable zero-age Main Sequence mass ranges of MS or RG companions, or the angular momentum and separation distributions of WD+WD pairs. A plausible means for determining the Delay Time Distribution (and, thus, the progenitor system) would be to compare the rate of SNe Ia events in a sample of galaxies to the rate of star formation in those galaxies.

Work on DTD has yielded mixed results. In the low-redshift regime, Maoz et al. (2011) showed a short delay time. In the medium range redshift regime, Sullivan et al. (2006) showed mixed delay times, but dominantly short delays. Strolger et al. (2010) showed that, in the high-redshift regime, the events preferred a longer delay time. Strolger suggested that one possible explanation of his results was a minimum metallicity – the universe had to achieve a certain metal content before the supernova events were possible. Physically, this means that potential White Dwarf progenitor stars need a level of metallicity to support an ultraviolet wind that allows steady mass accretion. This wind prevents rapid accretion that would trigger hydrogen and helium flashes on the surface, causing a nova, and also prevents accretion-triggered core-collapse supernova (Strolger et al. 2010; Kobayashi & Nomoto 2009).

Meng et al. (2011) decided to test this possible explanation for the mixed delay times seen in all redshift regimes. Their attempts at modeling the DTD mark the first attempts to merge all redshift observations into one explanation. Meng showed that as the metallicity

of the progenitor star increased, the mass of the companion star needed to increase. As determined previously in this section, as the mass of a star increases, the lifetime of the star decreases. Thus, it is proposed that metal rich progenitor stars (as mostly seen in the low- z universe) should produce SNe from young populations and the metal poor progenitors in the high- z universe should be highly delayed.

This provides a testable hypothesis, as the low- z universe, although dominated by metal-rich systems, includes a substantial population of metal poor systems as well. The test would be to see if metal rich systems are more prone to producing SNe Ia (by virtue of having both prompt and delayed SNe Ia) than currently metal poor systems which should only have delayed events. This could be very different from an “age effect” where young systems that are not necessarily metal rich (e.g. galaxy mergers) may produce more events than old systems that aren’t necessarily metal poor (e.g. early red ellipticals).

I attempt to show which characteristic (age or metallicity) is most representative of SN Ia hosts, either demonstrating the Meng et al. (2011) interpretation of metallicity dependent progenitors or validating one of the DTD interpretations of SN Ia production mechanisms.

CHAPTER II

Data: Groundwork to Present

2.1 Groundwork: The Nearby Galaxies Supernova Search Project

The Nearby Galaxies Supernova Search (NGSS) was designed to detect and study low-redshift supernovae of all types. This survey collected data from 1999 to 2001 using the 0.9-meter telescope and $8k \times 8k$ Mosaic North camera at Kitt Peak National Observatory (KPNO) just outside of Tucson, Arizona. The campaign consisted of four epochs as shown in Figure 2.1, surveying nearly 500 square degrees along the celestial equator and out of the galactic plane. At its time of completion, the Nearby Galaxies Supernova Search was the largest campaign for low- z supernovae.

In real time, NGSS discovered 42 supernovae, 30 of which were Type Ia. Beginning in 2005, the data was revisited by Gatton and WKU students using different temporal cadences between template and search-epoch images. This additional searching turned up an additional 29 potential Type Ia supernovae, bringing our total sample to 59 supernovae (Wolff 2011; Strolger 2003). Figure 2.1 shows the field coverage for NGSS. The square in the figure is roughly the size of the constellation Orion, approximately 50 square degrees, for comparison to the survey. The dotted lines are the outline of the galactic plane; one can

easily see that the plane was appropriately avoided in the survey.

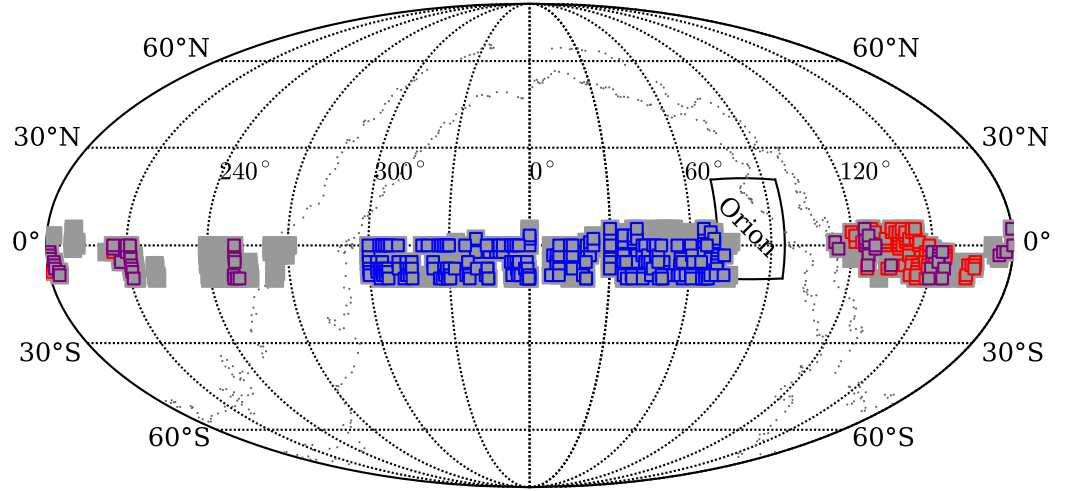


Figure 2.1: Sky coverage for the Nearby Galaxies Supernova Search. Each box indicates a single pointing of the 0.9m + Mosaic (~ 1 square degree) and are color coded by epoch, or visit. Gray is the template, blue is the second epoch, red is the third epoch, and purple is the fourth epoch.

2.2 Host Galaxy Spectra: Kitt Peak & Palomar

The sample of supernovae (and their hosts) collected from the NGSS project provides an excellent sample for investigating host galaxy environments, as nearly all are bright enough to adequately illuminate an optical spectrograph on a 4m class telescope within reasonable integration times.

Along with Schuyler Wolff, Dr. Louis-Gregory Strolger and I applied for and received four continuous semesters of observing time at the Mayall 4-meter telescope (with the Ritchey-Chretien Spectrograph) at Kitt Peak National Observatory, and the Hale 5.1-meter telescope (with the Double Spectrograph) at the Caltech/Palomar Observatory. Over this campaign, averaging 6 nights per semester, we obtained optical spectra of nearly all 59 of our SNe Ia and SN Ia candidates.

The setup for each observing run was nearly identical, and optimized to get excellent signal-to-noise ($S/N > 40$) at all wavelengths for the full spectral range ($3500\text{\AA} - 7500\text{\AA}$). At the Mayall telescope, we used the BL 181 grating (316 l/mm), alternating in first and second order, with the GG 455 and CuSO_4 blocking filters to optimize the red ($5000\text{\AA} - 7500\text{\AA}$) and blue ($3000\text{\AA} - 5500\text{\AA}$) spectral responses, respectively. At the Hale telescope, we could use two spectrograph setups simultaneously, and used the 316 l/mm and 300 l/mm gratings with no blocking filters.

Both observatories provided high S/N spectra ($S/N \geq 40$ per \AA) with a spectral resolution of $R \sim 1600$ (blue) and $R \sim 4000$ (red), or $< 6\text{ \AA}$ FWHM (blue) and $< 4\text{ \AA}$ FWHM (red). This is generally higher quality than the spectra obtained from the Sloan Digital Sky Survey.

I reduced each spectrum using standard IRAF two-dimensional long slit data reduction

techniques. All spectra were obtained near zero parallactic angle to minimize the differential atmospheric refraction. Images were flat-field corrected using quartz lamps illuminated at the position of the target objects. Wavelength dispersion solutions were determined from arc lamps, also imaged at the position of the target objects to minimize flexure in the spectrograph. Several spectrophotometric standards from the KPNO IIDS catalog were used to flux-calibrate our sample, with modest corrections for atmospheric extinction (airmass). Lastly, the observed spectra were de-redshifted by comparing prominent Ca H & K and/or HII features to the rest frame.

SN	A.K.A	Type	Host Galaxy	R.A. (2000)	Dec. (2000)	R (mag)
1999aq	William	Ia	Abell 0838[D80]019	09:38:10.8	-05:08:56	18.8
1999ar	Abhorsion	Ia	MCACSS J092016.00+00339.6	09:20:16.00	+00:33:39.6	19.7
1999au	Lucio	Ia	WOOTS J085858.01-072209.9	08:58:58.01	-07:22:09.9	19.2
1999av	Petruchio	Ia	GNX 087	10:55:49.7	-09:20:23	18.6
1999eo	Khadijih	Ia	Anon.	02:40:13.20	+04:54:55.4	19.6
1999ep	Lua	Ia	2MASXi J0441052-030034	04:41:04.76	-03:00:39.6	19.5
1999er	Joshua	II	MCG -01-08-008	02:47:06.88	-02:57:43.9	19.8
2000bn	Gabrielito	Ia	Anon.	09:35:41.15	+04:32:13.3	18.8
2000em	Animal	II-P	Anon.	00:35:29.82	-02:39:27.4	18.3
2000eq	Waldorf	Ia	Anon.	21:03:57.97	-09:41:31.8	20.5
2000ff	Swedish Chef	Ia?	Anon.	00:45:24.72	-03:16:47.2	19.5
2000fg	Janice	...	Anon.	01:24:31.36	-10:23:46.2	18.8
...	Barkley	...	Anon.	04:02:28.98	-10:07:04.5	18.0
...	George	...	LEDA 073961	01:26:21.66	-01:16:27.4	18.6
...	Laurel	...	Anon.	08:14:29.13	01:01:51.23	18.5
...	Xenia	...	Anon.	09:19:56.52	-02:12:04.34	19.7

Table 2.1: *NGSS* Supernovae and revisit-discovered supernovae used in Age/Metallicity comparison.

CHAPTER III

Tests of Environmental Effects

3.1 Determination of Metallicity and Ages in the Sample

One important factor in supernova production could be the dominant stellar population age of the host environment. Studies of the effects age has on supernova production have yet to yield consensus on dependencies. These approaches have been limited by simplifying assumptions on the ages of star formation histories of the parent sample (Mannucci et al. 2005). Another factor in supernova production is metallicity, or the ratio of elements in the star to hydrogen. Surprisingly, there have been no direct studies on the effects that the metallicity of the host environment has on SNe Ia production. However, it has been shown that the metallicity of the host environment is a good indicator of the progenitor system (Bravo & Badenes 2011). What needs to be determined is whether or not SNe Ia share a characteristic trend in metallicity or age, or both. Are these standard candles, somehow, “metal sensitive” or “age sensitive”?

I began my investigation with a routine called `EZ_Ages` (Graves & Shiavon 2008) which measures intensities of specific absorption features relative to a continuum in the galactic spectra, typically called Lick Indices (see Figure 3.2), and utilizes those values in an algo-

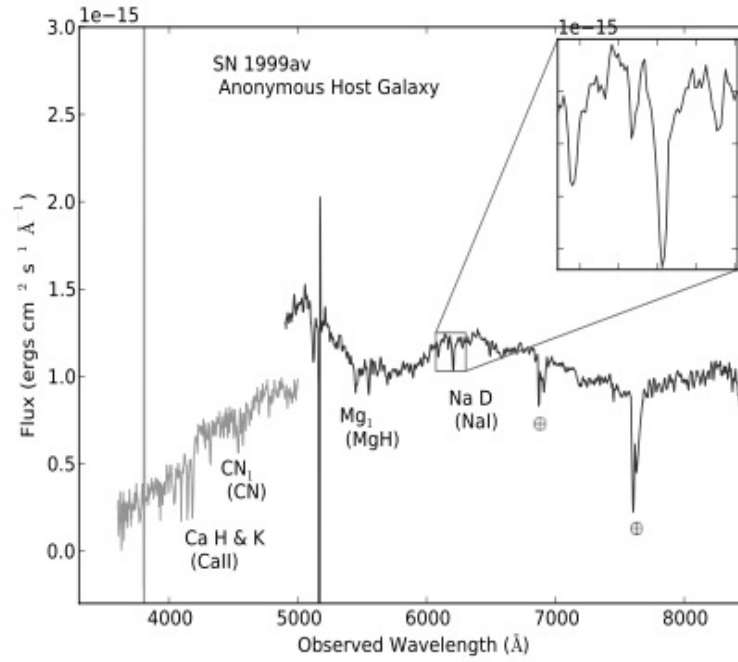


Figure 3.1: Spectrum of host galaxy of SN 1999av. This spectrum shows strong absorption features – Lick Indices – which passively tell about the chemical enrichment and ages of stars in the galaxy.

rithm that estimates the dominant age and metallicity of the galaxy. By measuring a key set of atomic and molecular lines, Lick indices allow a determination of the fraction of stars of different spectral types, and therefore, different lifetimes, as well as stars of different metallicities. The Lick indices allow us to simultaneously determine the dominant stellar age and metallicity in any galaxy. Before I could proceed with my analysis of the data, I ran some initial consistency checks to ensure that this program was performing properly over all parameter space, proving the legitimacy of its use.

3.1.1 The MILES Templates

MILES, or a Medium Resolution INT (Issac Newton Telescope) Library of Empirical Spectra is a stellar library developed for modeling stellar populations (Vazdekis et al. 2010). The library itself consists of ~ 1000 stars that were observed over a range of age and metallicity parameters, developed for stellar population synthesis modeling.

Stars are generally not formed in isolation, but rather in clusters of hundreds or even thousands. Such clusters form all their stars at approximately the same time and from the same gas cloud, meaning that all of the stars can be assumed to have the same age and metallicity. This is known as a “single stellar population” (SSP). The MILES library includes SSP stellar populations synthesis models for 304 combinations of age and metallicity. These models only include stars – no interstellar gas. This simplicity allowed us to have fewer parameters and made the templates easy to implement and interpret.

3.1.2 The Inadequacies of EZ_Ages

The test I devised for EZ_Ages was quite simple. I input a spectrum with a known age and a known metallicity and compared this to the age and metallicity of the EZ_Ages estimated output. The sample spectra used were obtained from Vazdekis’ online SSP model library. With EZ_Ages, I chose a sample of 35 of the available combinations of age and metallicity (7 metallicities [all that were available], and 5 ages over a span of approximately 9 billion years) to determine if it was the right fit for our purposes.

In the end, I was not satisfied with the performance of EZ_Ages. The program was best at interpolation, but not satisfactory in its ability to extrapolate outside of its internal points. This issue, coupled with the program methodology being poorly documented, led

Metallicity [Fe/H]	0.22	100%	11% Metallicity	23% Metallicity	100%	25% Metallicity
	0	100%	15% Age	0.34% Age	28% Metallicity	17% Age
	-0.4	100%	7.0% Age	7.1% Metallicity	3.4% Age	4.0% Metallicity
	-0.71	100%	100%	4.6% Age	4.1% Metallicity	2.8% Age
	-1.31	100%	100%	5.2% Age	1.0% Age	42% Age
	-1.71	100%	37% Metallicity	100%	22% Age	100%
	-2.32	100%	100%	100%	100%	100%
		0.7079	1.5849	3.1623	5.0119	10.0000
Age (Gyr)						

Figure 3.2: Plot of errors calculated between input parameters and parameters measured by EZ_Ages. Colors are based on error percentages of the greatest error (either age or metallicity, indicated in each box). Green boxes indicate errors below 20%, yellow boxes indicate errors between 20% and 50%. Red boxes are 100% errors, or failures. These are combinations that EZ_Ages could not output a measure of age or metallicity.

us to reject the EZ_Ages method.

Instead of a “black box” package, we opted to develop a code that would imitate EZ_Ages, but perform a more logical and systematic test. The code takes the square of the difference between our input host galaxy spectra and *every* Vazdekis SSP model. After iterating through all 304 models, the code reports the model that had the least square value, the dubbed “best fit.” This has the advantage of making use of the full observed spectrum, rather than specific spectral indices.

3.1.3 The CC-Test

To compute the “best fit” of our data, we chose a cross-correlation method, with the effective test statistic chosen to be the Minimum- χ^2 value, dubbed the CC_Test. The Minimum- χ^2 is calculated through Equation 3.6:

$$(3.1) \quad \chi^2 = \sum_{i=1}^n \frac{(O_i - E_i)^2}{E_i}$$

where χ^2 is the test statistic, O_i is the observed galactic spectrum, E_i is the MILES template, each evaluated over the “n” wavelengths of our observed spectra. The statistic is the summed squares of the residuals. The statistic for each combination of age and metallicity is compared, and the smallest statistic is the most likely age and metallicity combination for the data spectrum out of the entire synthetic set. Examples of comparisons can be seen in Figures 3.3 - 3.5. The $\Delta \log(f)$, the bottom region of each of the figures, is the measure of the statistic, and it should be obvious that the best fitting synthetic model has the smallest residual.

The information from Figures 3.3 - 3.5 make up individual data points on a greater contour plot, Figure 3.7. This figure is the Minimum- χ^2 contour plot for all tested MILES spectra. The region of maximum likelihood, the 1- σ region, is estimated by the size of the darkest contour around the Minimum- χ^2 point. A contour plot was made for each of the spectra. These contour plots are the basis for the results I attained.

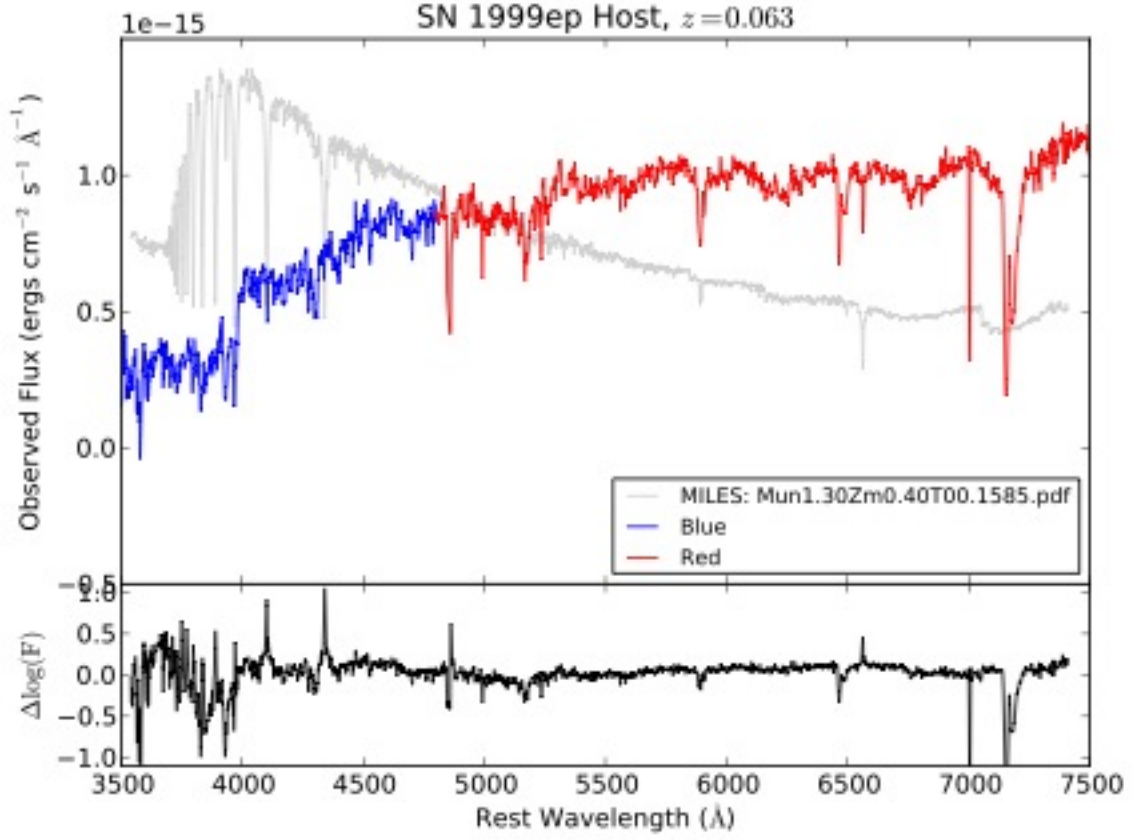


Figure 3.3: Illustration of the Minimum- χ^2 fit method between data and a MILES template spectrum. This plot shows a model that poorly fits the data, shown by its larger residuals in χ space.

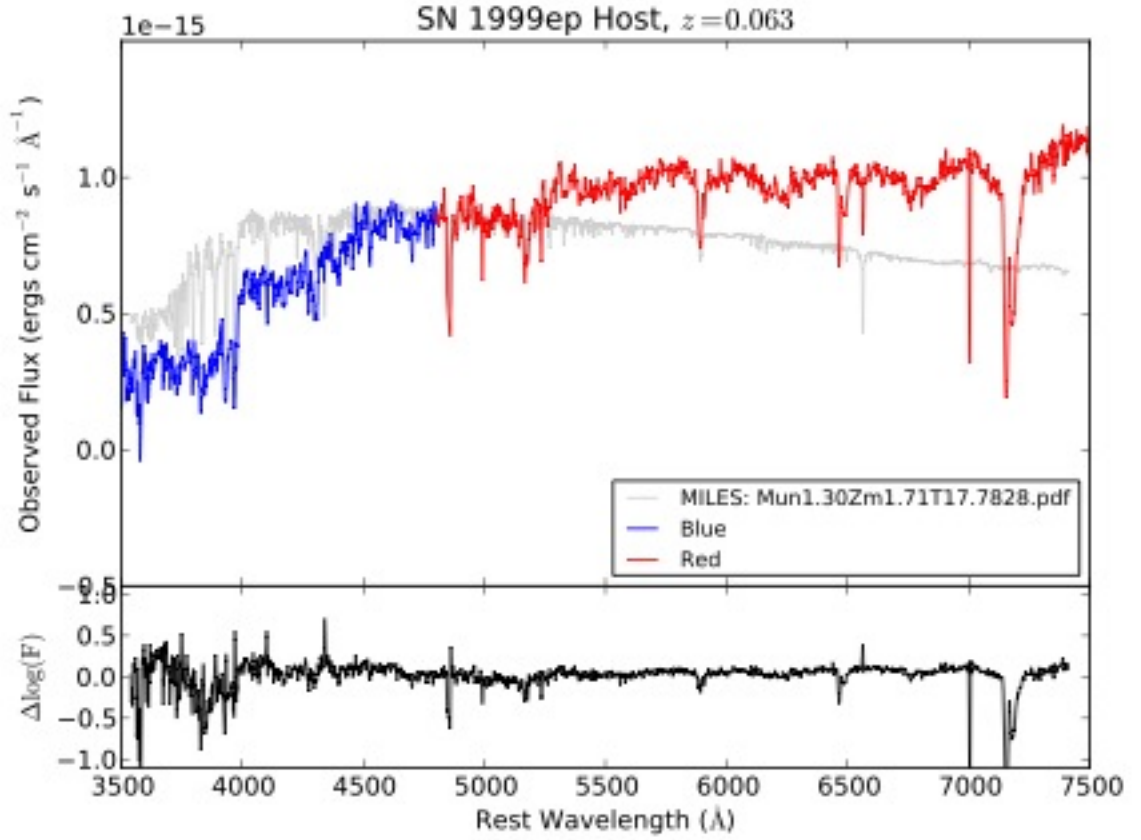


Figure 3.4: Illustration of the Minimum- χ^2 fit method between data and a MILES template spectrum. This plot shows a model that is a better fit to the data. The residuals in this comparison are much smaller than Figure 3.3.

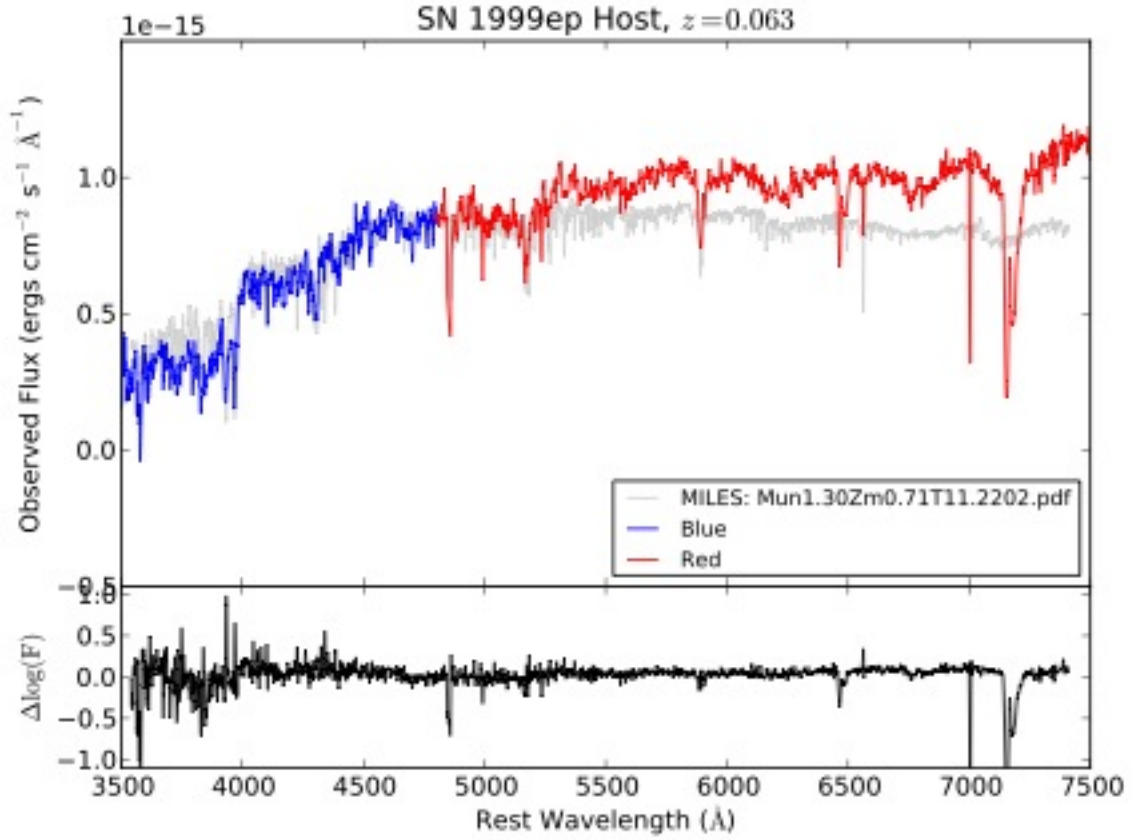


Figure 3.5: Illustration of the Minimum- χ^2 fit method between data and a MILES template spectrum. This plot shows a model that returned to be the minimum- χ^2 for the data for SN 1999ep. The residuals in χ space are the smallest out of every possible combination.

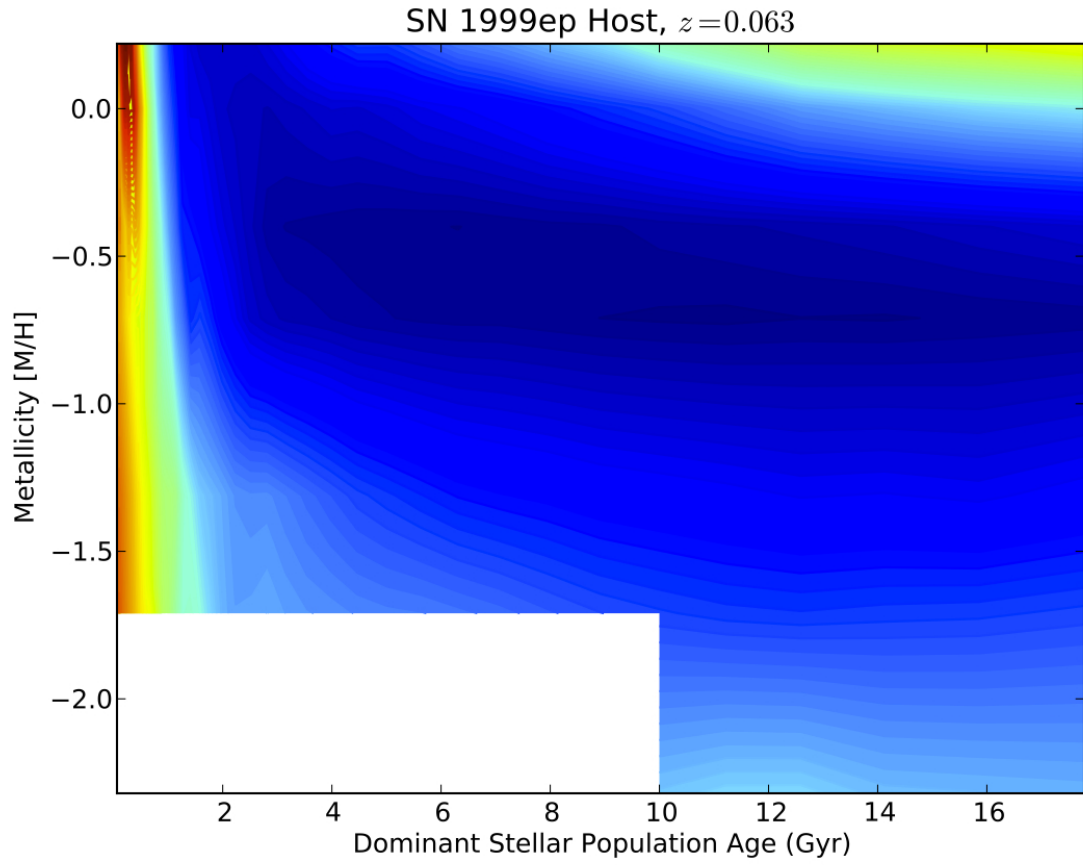


Figure 3.6: Contour plot, showing contour regions. The age and metallicity ranges were determined by analyzing the darkest region. The white region shows the untested region due to lack of MILES spectra.

CHAPTER IV

Conclusions

4.1 Results & Discussion

The best fits and $1\text{-}\sigma$ regions for our 16 spectra are shown in Figure 4.1. These are only conservative error estimates – in most cases the $1\text{-}\sigma$ regions were much smaller and less symmetric. Also shown is the region in which Meng et al. would predict the most SNe Ia would originate. From my comparison of data to synthetic spectra, I could not confirm Meng’s prediction. I found that the events measured had the full range of available metallicities. This result, however, does not rule out the possibility of a metallicity dependence; rather it implies a stronger dependence on age. Nearly 90% of our data points fell at an age greater than 9 Gyr. These results are seemingly more supportive of an older progenitor system, as indicated in Strolger et al. 2010.

The statistical certainty of my results appears to be at the 75% level. These results are limited by the sample size and, possibly, by the method. We could potentially learn more by increasing our sample size to contain more of the total sample or by changing our library type (i.e. using PEGASE.2 models instead of MILES, to be discussed in Section 4.1.2). However, we have a sample size large enough to believe that the interpretation is

statistically robust.

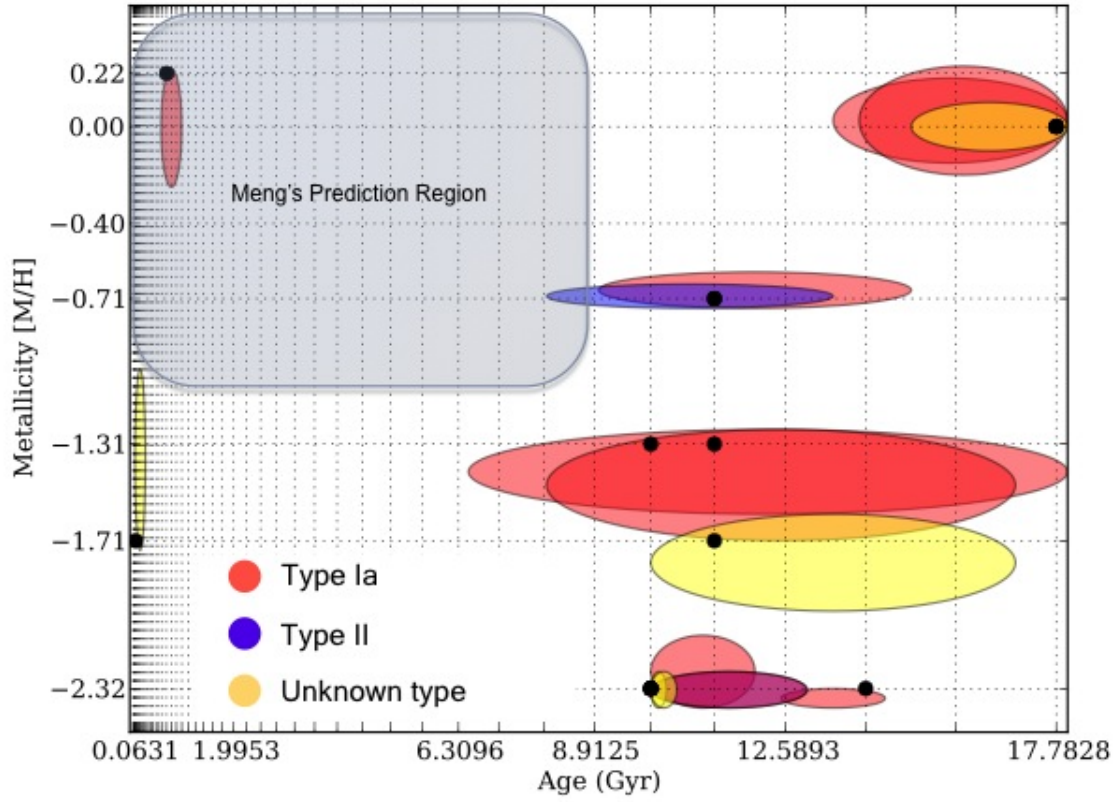


Figure 4.1: Final plot with an estimation of Meng's prediction region overlaid. Upper left of the plot would include young, star-forming galaxies. Upper right of the plot would include old, star-forming galaxies. Bottom left of the plot would be unusual galaxies – young, but lacking in the metal content that one would expect with the increased metal abundances in the universe (Note that this region was generally untestable due to the lack of MILES spectra). Bottom right of the plot would contain old, dying red galaxies that did not undergo many phases of star-formation.

4.1.1 Table of Ages and Metallicities

Host	Age (Gyr)	High Age (Gyr)	Low Age (Gyr)	Metallicity [M/H]	High Metallicity [M/H]	Low Metallicity [M/H]
99aq	0.7079	1.00	0.60	0.22	0.24	-0.25
99ar	14.1254	14.5	12.5	-2.32	-2.32	-2.40
99au	17.7828	18.0	14.0	0.00	0.20	-0.15
99av	10.0000	18.0	6.50	-1.31	-1.25	-1.60
99eo	10.0000	18.0	10.0	-2.32	-2.10	-2.40
99ep	11.2202	12.0	9.00	-0.71	-0.60	-0.75
99er	11.2202	15.0	8.00	-0.71	-0.65	-0.75
00bn	11.2202	13.5	8.00	-1.31	-1.25	-1.71
00em	10.0000	17.0	10.0	-2.32	-2.25	-2.40
00eq	17.7828	13.0	14.0	0.00	0.25	-0.20
00ff	10.0000	18.0	10.0	-2.32	-2.24	-2.40
00fg	17.7828	13.0	15.0	0.00	0.10	-0.10
Barkley	11.2202	18.0	10.0	-1.71	-1.60	-2.00
George	0.1122	0.30	0.10	-1.71	-1.00	-1.75
Laurel	10.0000	10.3	10.0	-2.32	-2.25	-2.25
Xenia	10.0000	10.5	10.0	-2.32	-2.25	-2.25

Table 4.1: Numerical findings from Age/Metallicity comparison.

4.1.2 Future Work

I have analyzed 16 host spectra out of a sample of approximately 60 available spectra. The obvious next step is to attain ages and metallicities of the remaining test sample. I anticipate that the remaining sample will either help to fill out the final plot or confirm the stronger age dependence of these events.

In addition, it would be interesting to explore the possible use of potentially better galactic models. The SSP models are more suited for modeling globular clusters than spiral galaxies. In spiral galaxies, there is constant star formation and there are prominent gas clouds, though useful in this current regard, are highly unphysical in that they do not include gas content nor do they account for multiple age populations. It is incredibly im-

portant to account for gases present in the galaxy because the light from the stars in the galaxy interacts with the gas, adding absorption and emission lines to the galactic spectra. Additionally, the gas content provides an initial rate of star formation. Young, star-forming galaxies would have more abundant gas clouds than old galaxies. Because of the presence of gas absorption and emission lines, star-forming galaxies are more likely to match with the wrong SSP model. These galaxies have many more features than we are testing for, both in the emission and absorption, so the simplistic cross-correlation test is less robust than the ideal test. One set of models that would be worth looking into would be the `PEGASE.2` models.

Another place for improvement lies in the errors, specifically, the systematic error. One question that we have yet to fully flesh out is this: How does the signal to noise ratio affect the robustness of the cross-correlation test? It is inevitable that we attain error in any measurement. The issue is not necessarily the signal-to-noise ratio, though it is always a place for improvement. We do not fully know how the noise in the true data affected the template fittings. Additionally, spectral combining could be a source of error. We took multiple observations of the same galaxy, and combined the spectra to increase the signal-to-noise ratio. However, when we only have three observations, and many extraneous sources (bad pixels, cosmic rays, etc.) could taint our data, we opted to bias low by rejecting the highest pixel, avoiding fake signal. This may have created false features in the spectra. More investigation into the process of spectral combining is required to minimize these errors.

The NGSS was a precursor to the Sloan Digital Sky Surveys. The surveys were designed to look at galaxies, but had a piggy-back supernova detection operation. All of the SDSS targets are low- z , within a comparable redshift to NGSS collection region. SDSS-II

detected 517 supernovae and 247 were spectroscopically identified as Type Ia (Dilday et al. 2010). An excellent step up for my project would be to analyze these supernovae from SDSS-II using the more robust PEGASE.2 models, should they prove to be effective. This would bring our statistical error to 6%, near the $2\text{-}\sigma$ certainty region.

The effects of age and metallicity on SNe Ia production are important aspects to take into consideration when determining the progenitor system of the events. However, these are not the only particulars that play a part in that determination. A complimentary project has explored ways to determine SN rates. These investigations will be included along with the results discussed in this thesis in a forthcoming publication.

Scientists continue to search and observe and calculate. Time and again, we are met with conflict, contradiction, and confusion instead of the comfort and clarity for which we yearn. Is there hope for us as we seek to understand the nature of Dark Energy, this mysterious force so intricately and cleverly integrated into the very fabric of the universe? Time can only tell and it is traveling as fast as it can. As E. P. Hubble wrote of the initial quest to measure cosmic expansion,

“Thus the explorations of space end on a note of uncertainty. And necessarily so. We are, by definition, in the very center of the observable region. We know our immediate neighborhood rather intimately. With increasing distance, our knowledge fades, and fades rapidly. Eventually, we reach the dim boundary – the utmost limits of our telescopes. There, we measure shadows, and we search among ghostly errors of measurement for landmarks that are scarcely more substantial. The search will continue. Not until the empirical resources are exhausted, need we pass on to the dreamy realms of speculation.”

The Realm of the Nebulae

BIBLIOGRAPHY

- Bravo, E., & Badenes, C. 2011, Monthly Notices of the Royal Astronomical Society, 414, 1592
- Filippenko A. V. 1997, Annual Review of Astronomy and Astrophysics, 35, 309
- Gallagher et al. 2008, The Astrophysical Journal, 685, 749
- Graves, G. & Shiao. 2008, The Astrophysical Journal Supplement, 177, 446
- Hamuy et al. 2000, The Astronomical Journal, 120, 1479
- Howell et al. 2009, The Astrophysical Journal, 691, 661
- Kobayashi C., Nomoto K., 2009, The Astrophysical Journal, 707, 1466
- Maoz, D., Mannucci, F., Li, W., Filippenko, A. V., Della Valle, M., & Panagia, N. 2011, Monthly Notices of the Royal Astronomical Society, 412, 1508
- Meng, Xiang Cun; Li, Zhong Mu; Yang, Wu Ming 2011, Publications of the Astronomical Society of the Pacific, 63, 31
- Phillips M. M. 1993, The Astrophysical Journal, 431, 105
- Pinto & Eastman 2000, The Astrophysical Journal, 530, 744
- Perryman, M. A. C., et al. 1997, Astronomy and Astrophysics, 323, 49
- Riess, A. . et al. 1998, The Astronomical Journal, 116, 1009
- Strolger, L. -G., Dahlen, T., & Reiss, A. G. 2010, The Astrophysical Journal, 713, 32
- Sullivan, M., et al. 2006, The Astrophysical Journal, 648, 868
- Timmes et al. 2003, The Astrophysical Journal, 590, 83
- Van Dyk, S. D., Li, W., & Filippenko, A. V. 2003, Publications of the Astronomical Society of the Pacific. 115, 1259
- Vazdekis et al. 2010, Monthly Notices of the Royal Astronomical Society, 404, 1639
- Wolff, S. G. 2010, WKU Honors Thesis